



Contents lists available at ScienceDirect

Bioorganic & Medicinal Chemistry Letters

journal homepage: www.elsevier.com/locate/bmcl

Monosubstituted γ -lactam and conformationally constrained 1,3-diaminopropan-2-ol transition-state isostere inhibitors of β -secretase (BACE)

Kenneth M. Boy^{a,*}, Jason M. Guernon^a, Jianliang Shi^a, Jeremy H. Toyn^b, Jere E. Meredith^b, Donna M. Barten^b, Catherine R. Burton^b, Charles F. Albright^b, Jovita Marcinkeviciene^{c,†}, Andrew C. Good^{d,‡}, Andrew J. Tebben^e, Jodi K. Muckelbauer^f, Daniel M. Camac^f, Kimberley A. Lentz^g, Joanne J. Bronson^a, Richard E. Olson^a, John E. Macor^a, Lorin A. Thompson III^a

^a Department of Neuroscience Discovery Chemistry, Research and Development, Bristol-Myers Squibb, 5 Research Parkway, Wallingford, CT 06492, USA

^b Department of Neuroscience Discovery Biology, Research and Development, Bristol-Myers Squibb, 5 Research Parkway, Wallingford, CT 06492, USA

^c Department of Chemical Enzymology, Research and Development, Bristol-Myers Squibb, 311 Pennington-Rocky Hill Road, Pennington, NJ 08534, USA

^d Department of Computer Assisted Drug Design, Research and Development, Bristol-Myers Squibb, 5 Research Parkway, Wallingford, CT 06492, USA

^e Department of Computer Assisted Drug Design, Research and Development, Bristol-Myers Squibb, 3551 Lawrenceville Road, Princeton, NJ 08648, USA

^f Department of Protein Science and Structure, Research and Development, Bristol-Myers Squibb, 3551 Lawrenceville Road, Princeton, NJ 08648, USA

^g Department of Pharmaceutical Candidate Optimization: Metabolism and Pharmacokinetics, Research and Development, Bristol-Myers Squibb, 5 Research Parkway, Wallingford, CT 06492, USA

ARTICLE INFO

Article history:

Available online 30 June 2011

Keywords:

Alzheimer's

Beta-secretase

BACE

Transition-state isostere

ABSTRACT

The synthesis, evaluation, and structure–activity relationships of a class of γ -lactam 1,3-diaminopropan-2-ol transition-state isostere inhibitors of BACE are discussed. Two strategies for optimizing lead compound **1a** are presented. Reducing the overall size of the inhibitors resulted in the identification of γ -lactam **1i**, whereas the introduction of conformational constraint on the prime-side of the inhibitor generated compounds such as the 3-hydroxypyrrolidine inhibitor **28n**. The full in vivo profile of **1i** in rats and **28n** in Tg 2576 mice is presented.

© 2011 Elsevier Ltd. All rights reserved.

Alzheimer's disease (AD) is a progressive neurodegenerative disease which currently affects 5 million Americans.¹ Since age is the single best predictor of AD, the growing elderly population is expected to cause the ranks of the affected to grow dramatically (est. 16 million cases in 2050) over the coming decades.² Current approved therapies for AD, including acetylcholinesterase inhibitors and NMDA antagonists, do not slow the progression of AD, and are only palliative in nature.³ Therapies which would directly modify the course of the disease are urgently needed, and would benefit patients, their families and their caregivers.

The hallmark features of an AD-affected brain are neurofibrillary tangles composed of hyperphosphorylated tau and plaques of deposited beta-amyloid (A β) peptide. While the precise sequence of events that lead to the development of AD is still under active investigation, the dominant amyloid hypothesis⁴ holds that

* Corresponding author. Tel.: +203 677 6278, fax: +203 677 7702.

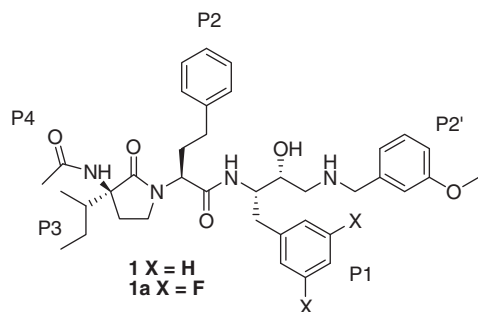
E-mail address: boyk@bms.com (K.M. Boy).

[†] Present address: Novartis Institutes for BioMedical Research, 9 Cambridge Center, Cambridge, MA 02142, USA.

[‡] Present address: Genzyme Pharmaceuticals, 153 Second Avenue, Waltham, MA 02451, USA.

the 42 amino acid form of A β (A β 42) derived from proteolysis of the amyloid precursor protein (APP) is toxic and is causative of the downstream disease cascade. Originally the insoluble plaques, composed of A β monomers, were hypothesized to be the toxic agent responsible for neurodegeneration. However, recent work has suggested that the soluble oligomers of A β 42 are highly toxic to neurons⁵ and are more likely to be the cause of the neurodegeneration seen in the disease. Inhibitors of either β -secretase or γ -secretase, two enzyme activities responsible for A β production, would be expected to slow disease progression by lowering the pool of toxic, soluble A β . BACE-1 cleaves APP to produce the N-terminus of the A β peptides, which is the first step in APP processing.^{6,7} Removal of BACE-1 activity by chemical inhibition or gene deletion leads to complete blockage of A β production. Given that BACE is mainly expressed in the CNS and that BACE knockout mice are viable, inhibitors of BACE-1 are hypothesized to be safe, disease-modifying agents for the treatment of AD.

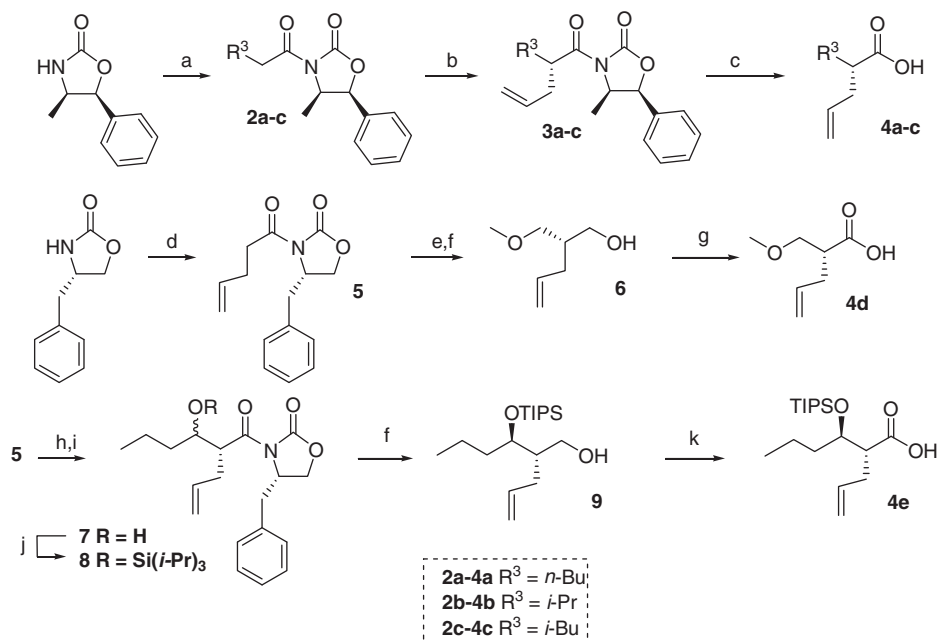
Previously,⁸ the development of γ -lactam peptidomimetic BACE inhibitors (e.g., **1a**) was described. Key features of this molecule included the 1,3-diaminopropan-2-ol transition state isostere and the conformational constraint inherent in the P3-bearing γ -lactam.



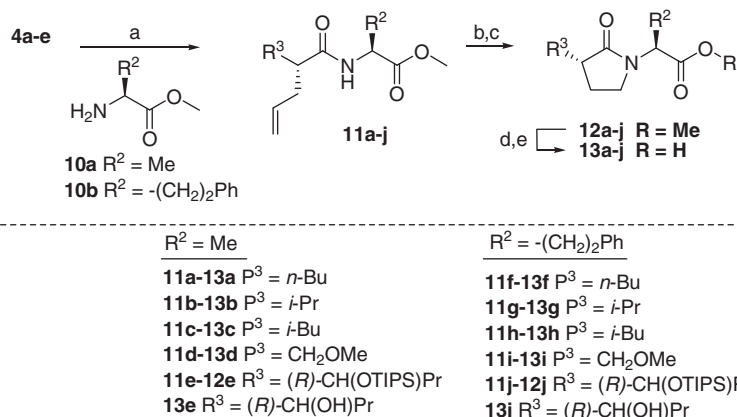
While **1a** has acceptable potency and selectivity over other aspartyl proteases (i.e., cathepsin D, cathepsin E and pepsin), the large molecular weight and modest Caco-2 permeability were key issues that needed to be addressed to make more drug-like

molecules. In this Letter, we describe our efforts to maintain potency with smaller and more permeable molecules. Initially, three main strategies were employed: (1) elimination of the acetamide functionality from the γ -lactam, (2) reduction of the size of the P2 homophenylalanine side chain, and (3) potency enhancement via incorporation of an additional conformational constraint on the prime side of the transition-state isostere.

The synthons for the synthesis of the γ -lactam portion of the target compounds are described in Scheme 1. Utilizing two related methods, the intermediate α -allylcarboxylic acids **4a–c**, as well as the α -allylcarboxylic acids **4d–e** started from acylated Evans' auxiliaries. Stereocontrolled allylation of **2a–c** afforded the intermediates **3a–c**, with excellent diastereocontrol. Hydrolysis of the auxiliary with lithium peroxide provided carboxylic acids **4a–c**. The oxygenated carboxylic acid derivatives **4d** and **4e** were prepared via the pentenoylated auxiliary **5** (opposite sense of stereocontrol). This intermediate was deprotonated with NaHMDS and alkylated with bromomethyl methyl ether and reductive re-



Scheme 1. Synthesis of monosubstituted γ -lactam precursors **4a–e**. Reagents and conditions: (a) *n*-BuLi, R³CH₂C(O)Cl, THF, –78 °C to rt, 38–87%; (b) NaHMDS, allyl bromide, THF, –78 °C, 41–66%; (c) LiOH, H₂O₂, H₂O, THF, 0 °C to rt, 30–68%; (d) *n*-BuLi, 4-pentenoyl chloride, THF, –78 °C to rt, 97%; (e) NaHMDS, bromomethyl methyl ether, THF, –78 °C; (f) LiBH₄, THF, MeOH, 0 °C to rt, 79% from **8**; (g) Jones reagent, acetone, rt, 37%, three steps from **5**; (h) (1) **5**, *i*-Pr₂NEt, CH₂Cl₂, Bu₂BOTf, 0 to –78 °C, (2) Et₂AlCl, hexane, CH₂Cl₂, –78 °C, PrCHO, (3) add (2) to (1), –78 °C; (i) 5:1 MeOH:30% H₂O₂, 40% from **5**, dr ~4:1; (j) 2,6-lutidine, CH₂Cl₂, TIPSOTf, 0 °C, then separate diastereomers, 89%; (k) Dess–Martin periodinane, CH₂Cl₂, then NaClO₂, NaH₂PO₄, 2-methylbutene, *t*-BuOH, H₂O, >90%.



Scheme 2. Synthesis of monosubstituted γ -lactam carboxylic acid synthons **13a–j**. Reagents and conditions: (a) **4a–e**, HATU, *N*-methylmorpholine, DMF, 48–90%; (b) O₃, MeOH, then PPh₃; (c) Et₃SiH, TFA, CH₂Cl₂, 0 °C, 71–96% from **11**; (d) for **11e** and **11j**: TBAF, THF, rt; (e) 2 M LiOH, THF, rt, >90% from **12**.

removal of the auxiliary afforded alcohol **6**. Oxidation with Jones reagent supplied carboxylic acid **4d**. To produce intermediate **4e**, an aldol reaction between the boron enolate of **5** and butyraldehyde activated with diethyl aluminum chloride afforded **7**. The resulting alcohol was protected as the TIPS ether. Removal of the auxiliary with lithium borohydride gave alcohol **9**, which was oxidized by sequential treatment by Dess–Martin periodinane and buffered sodium hypochlorite to supply the carboxylic acid **4e**.

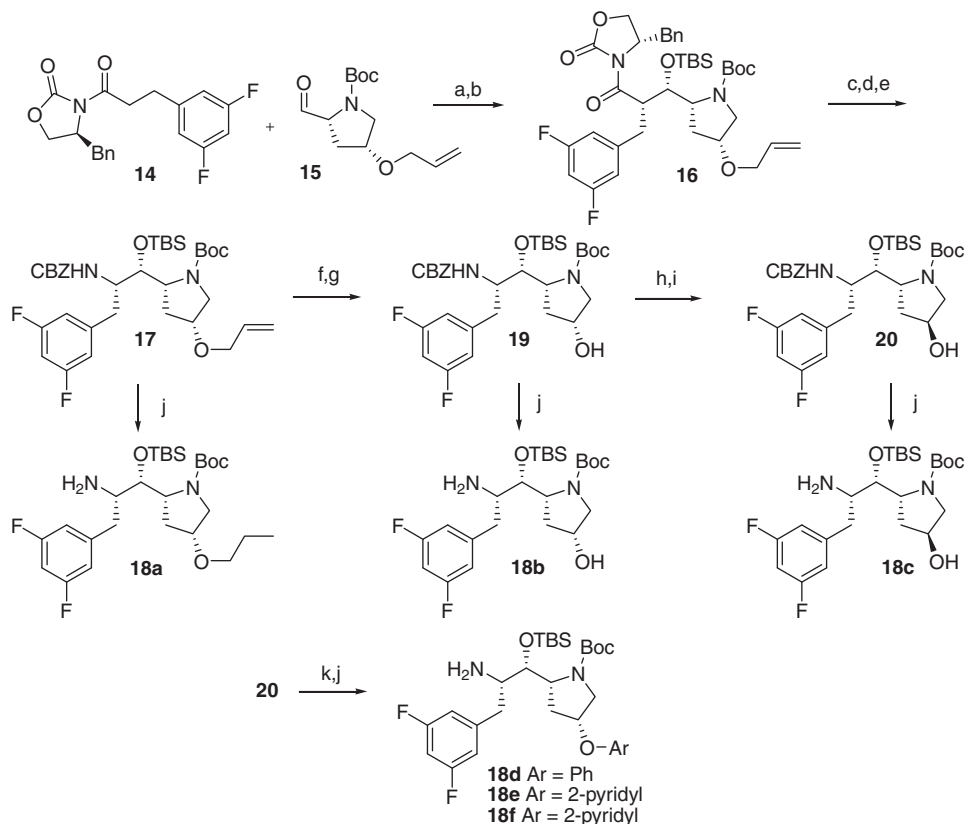
In Scheme 2, the acids **4a–e** were then converted to the γ -lactam carboxylic acids **13a–e** by condensation with P2-bearing α -aminoesters (**10a–b**), using HATU as the coupling agent, to yield the γ -lactam precursors **11a–j**. Ozonolysis of **11a–j**, followed by reduction of the resulting hemiaminal with triethylsilane in TFA formed the γ -lactams **12a–j**. Saponification with lithium hydroxide afforded the carboxylic acids **13a–j**.

The syntheses of protected pyrrolidine-based P1–P2' diamines **18a–f** utilized the previously described protected aldehyde **15**⁹ (Scheme 3). Stereocontrolled aldol addition of the boron enolate of (*S*)-4-benzyl-3-(3-(3,5-difluorophenyl)propanoyl)oxazolidin-2-one (**14**) with protected aldehyde **15** followed by protection of the newly formed alcohol as a TBS ether afforded compound **16**. During installation of the TBS group, the use of 2,6-lutidine in both the substrate solution as well as in the TBS triflate solution was required to avoid undesired cleavage of the *N*-Boc protecting group on **15**. The chiral auxiliary was then hydrolyzed using lithium peroxide, and the resulting carboxylic acid was reacted with DPPA to effect a Curtius rearrangement. The resulting isocyanate was trapped by benzyl alcohol to produce the *N*-CBZ-protected intermediate **17**. While direct hydrogenation of **17** afforded the primary amine **18a**, the removal of the allyl group with Wilkinson's catalyst

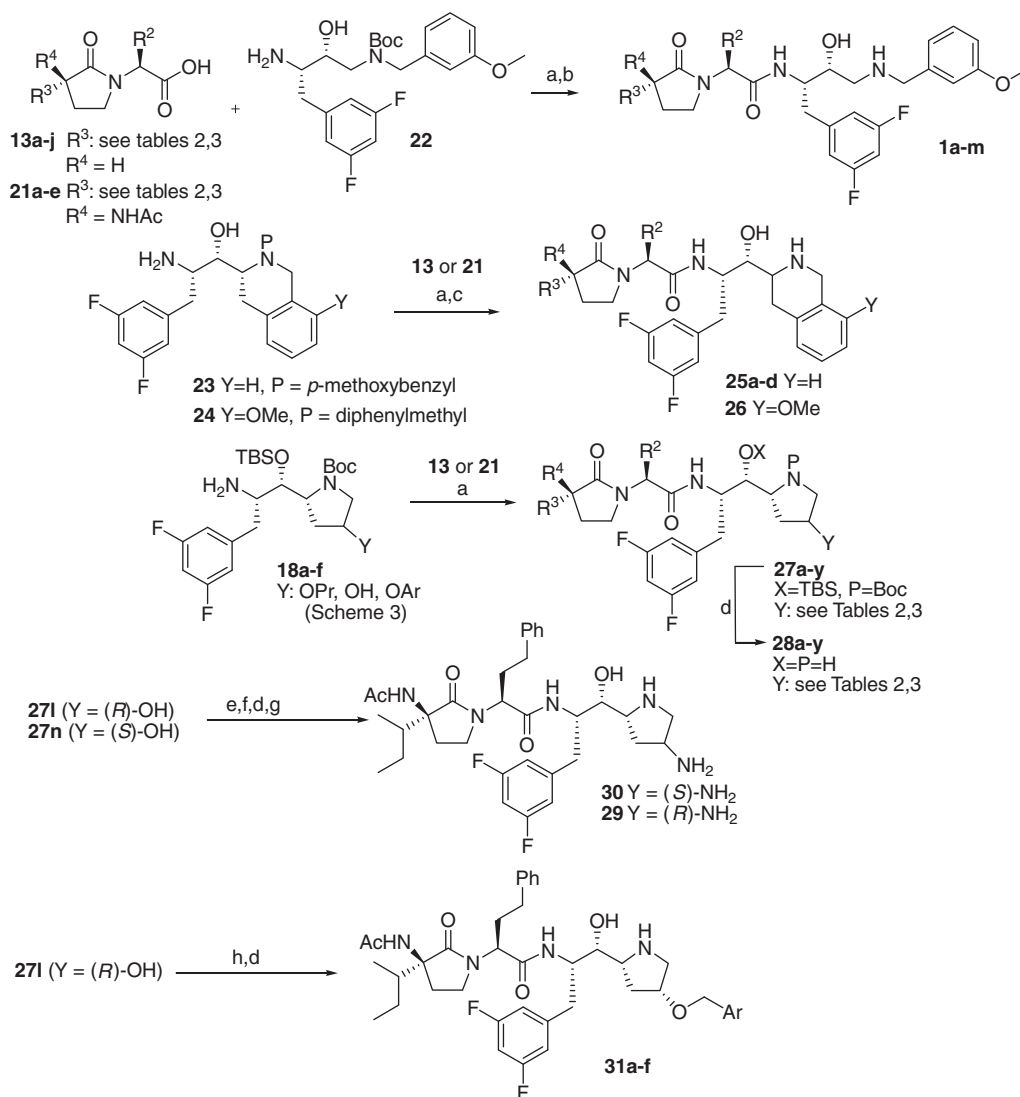
followed by KMnO_4 yielded the versatile alcohol **19**. This alcohol was hydrogenated to provide directly the amine **18b**. The amine **18c** containing the epimeric alcohol was generated by Mitsunobu inversion (to form alcohol **20**) followed by hydrogenation. Additionally, alcohol **20** was reacted under Mitsunobu conditions to obtain, after hydrogenation, aryloxy derivatives **18d–f**.

The final inhibitors were prepared as is shown in Scheme 4. Condensation of the lactam carboxylic acids **13a–j** (Scheme 2) and **21a–e**¹⁰ with the known amino-alcohol **22**¹⁰ using HATU provided, after *N*-Boc deprotection with TFA, the 1,3-diaminopropan-2-ol derivatives **1a–m**. Likewise, **13a–j** (Scheme 2) and **21a–e**¹⁰ were condensed with the elaborated amines **23**⁸ and **24**⁸ to afford, after hydrogenation, the tetrahydroisoquinoline (THIQ) compounds **25a–d** and **26**⁸. The proline derivatives **28a–y** were prepared by condensing carboxylic acids **13a–j** (Scheme 2) and **21a–e**¹⁰ with amines **18a–f** (Scheme 3) with subsequent hydrolysis of both the TBS ether and the *N*-Boc protecting groups with HCl in dioxane. Amino analogs **29** and **30** were generated from the protected pyrrolidinol-lactams **27l** and **27n** by azide displacement of the corresponding mesylates, with inversion of configuration. Hydrolysis of the TBS ether and *N*-Boc carbamate with HCl followed by hydrogenation of the azide yielded the final compounds **29** and **30**. The benzyloxy derivatives **31a–f** were furnished by the alkylation of **27l** with various benzyl bromides and (bromomethyl)pyridines.

The predominant feature of our 1,3-diaminopropan-2-ol isostere chemotype (i.e., **1a**) is a *gem*-disubstituted γ -lactam group. As observed from the X-ray crystal structure of the des-fluoro analog **1**,⁸ the lactam orients the P3 isobutyl substituent into the S3 pocket normally occupied by the valine side-chain in the natural substrate (interaction with I110 and G230), while projecting the acetamide



Scheme 3. Synthesis of functionalized pyrrolidine-based 1,3-diaminopropan-2-ol fragments **18a–f**. Reagents and conditions: (a) (*S*)-4-benzyl-3-(3-(3,5-difluorophenyl)propanoyl) oxazolidin-2-one, Bu_2BOTf , DIPEA, CH_2Cl_2 , -78°C to rt, 74%, dr 3:1; (b) 2,6-lutidine, TBSOTf, CH_2Cl_2 , see text, 78%; (c) LiOH , H_2O_2 , $\text{THF}/\text{H}_2\text{O}$, 73%; (d) DPPA, DIPEA, PhMe, 75°C ; (e) PhCH_2OH , 75°C , 77% over two steps; (f) Wilkinson's catalyst, EtOH/water , reflux; (g) KMnO_4 , EtOH , pH 10 buffer, rt, 60% over two steps; (h) DEAD, PPh_3 , THF, 4-nitrobenzoic acid, rt, 83%; (i) K_2CO_3 , MeOH, rt, 58%; (j) H_2 , Pd/C, MeOH, 51–91% for **18a–c**, 23–66% over two steps for **18d–f**; (k) DEAD, PPh_3 , THF, ArOH, rt.



Scheme 4. Synthesis of final compounds **1**, **25a–d**, **26**, and **28–31**. Reagents and conditions: (a) HATU, *N*-methylmorpholine, DMF; (b) TFA, CH_2Cl_2 , 48–81% over two steps; (c) H_2 , Pd/C, MeOH, HOAc, 31–75% over two steps; (d) 4 N HCl in dioxane, water, 29–34% from **18**, 8–32% from **27l**; (e) MsCl, pyridine; (f) NaN_3 , DMF, 70 °C, 67–100% over two steps; (g) H_2 , Pd/C, MeOH, 24–32% over two steps; (h) 2 equiv NaHMDS, ArCH_2Br .

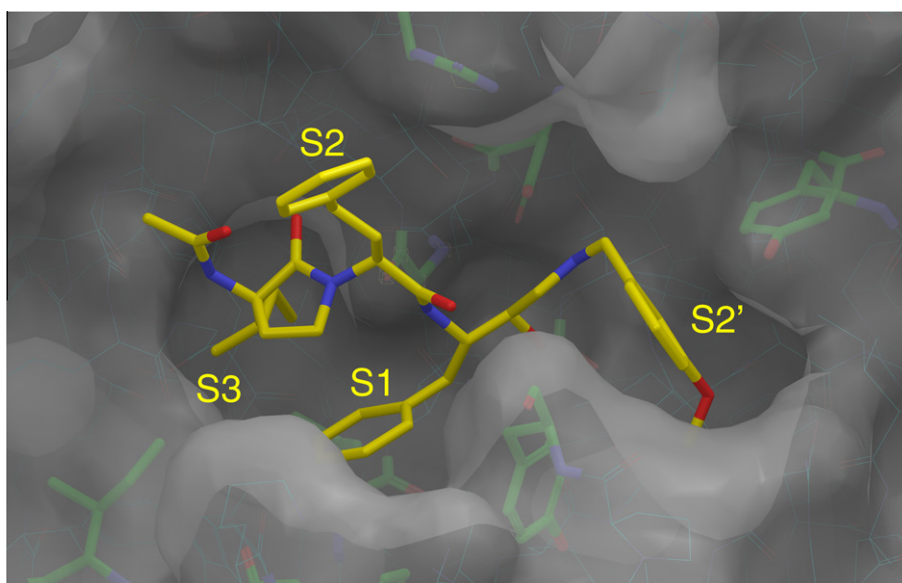
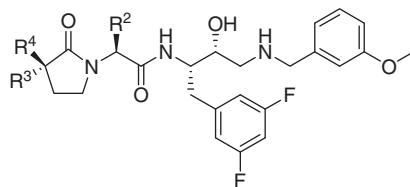


Figure 1. X-ray crystal structure of **1** in the BACE-1 active site.

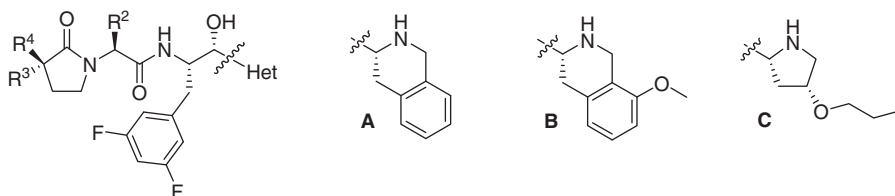
Table 1



Compound	R ⁴	R ³	R ²	HPLC ^a IC ₅₀ (nM)	HEKsw ^b IC ₅₀ (nM)
1a	NHAc	sBu	(CH ₂) ₂ Ph	6.1	n.d.
1b^c	NHAc	CH ₂ cPr	(CH ₂) ₂ Ph	11	10
1c	H	nBu	(CH ₂) ₂ Ph	38	350
1d	H	iPr	(CH ₂) ₂ Ph	75	220
1e	H	iBu	(CH ₂) ₂ Ph	20	240
1f	H	CH ₂ OMe	(CH ₂) ₂ Ph	32	210
1g	H		(CH ₂) ₂ Ph	5.2	90
1h	NHAc	CH ₂ cPr	Me	46	27
1i	H	nBu	Me	60	81
1j	H	iPr	Me	170	240
1k	H	iBu	Me	89	67
1l	H	CH ₂ OMe	Me	480	400
1m	H		Me	68	27

^a n = 2.^b n = 4.^c **1b** is the des-fluoro analog at P1.

Table 2



Compound	R ⁴	R ³	R ²	Het	HPLC ^a IC ₅₀ (nM)	HEKsw ^b IC ₅₀ (nM)
25a	NHAc	iBu	(CH ₂) ₂ Ph	A	8.6	9.5
25b	NHAc	sBu	(CH ₂) ₂ Ph	A	54	110
25c	H	nBu	(CH ₂) ₂ Ph	A	n.d.	1400
25d	H	nBu	Me	A	n.d.	720
26	NHAc	sBu	(CH ₂) ₂ Ph	B	4.2	20
28a	NHAc	iBu	(CH ₂) ₂ Ph	C	1.4	2.0
28b	NHAc	sBu	(CH ₂) ₂ Ph	C	2.6	2.7
28c	H	nBu	(CH ₂) ₂ Ph	C	19	84
28d	H	iPr	(CH ₂) ₂ Ph	C	21	99
28e	H	iBu	(CH ₂) ₂ Ph	C	5.7	69
28f	H	CH ₂ OMe	(CH ₂) ₂ Ph	C	23	89
28g	H		(CH ₂) ₂ Ph	C	4.7	48
28h	H	nBu	Me	C	87	68
28i	H	iPr	Me	C	160	390
28j	H	iBu	Me	C	35	110
28k	H		Me	C	70	55

^a n = 2.^b n = 4.

group toward S4 (Fig. 1). The homophenylalanine sidechain has hydrophobic contacts with T72 and R235 within S2, while the P1 benzyl group interacts with F108 and L30 at the bottom of the S1 pocket. The 1,3-diaminopropan-2-ol transition-state isostere fragment forms the key H-bonds with D32 and D228 (from the

ligand alcohol and ammonium moieties, respectively), while the *m*-methoxybenzyl group is in contact with Y71 and Y198 within the S2' binding pocket. In considering how the size of these inhibitors could be reduced, we made molecular models of several potent γ -lactam inhibitors using information from the previously

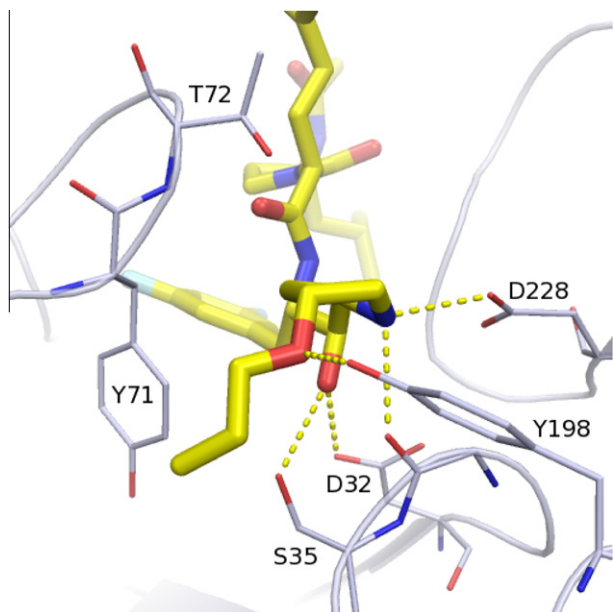


Figure 2. Model of **28a** docked into the BACE-1 active site.

described X-ray structure.¹¹ We also solved additional moderate-resolution crystal structures (unpublished results). Together, these data suggested that two binding conformations (rotamers) for the acetamide functionality were possible, with the T232 carbonyl interacting with the NHAc in only one pose. This suggested that the loss in potency upon removing this entire group ($R^4 = \text{NHAc}$) would be modest. Compounds made according to this hypothesis were screened for BACE-1 enzyme inhibition¹² and for their ability to inhibit A β 1-40 production in cultured HEKsw cells.¹³ A four- to six-fold loss in BACE-1 potency in the enzyme assay was observed for the monosubstituted γ -lactam **1c** (38 nM) versus the reference disubstituted lactams **1a** and **1b** (Table 1). Further exploration of the P3 group revealed that branching of R^3 was tolerated (**1d**), with a slight improvement in potency seen the isobutyl analog **1e** (20 nM). Ether analog **1f** had similar potency to **1c**. Among the cohort of the monosubstituted lactams ($R^4 = \text{H}$), alcohol **1g** was superior in both in vitro (HPLC IC_{50}) and cellular (HEKsw IC_{50}) potency (5.2 and 90 nM, respectively). To further reduce the molecular weight of the inhibitors, the homophenylalanine P2 moiety was replaced with alanine (**1i–m**). Compounds **1i–k** were a modest two- to five-fold less potent than the homophenylalanine derivatives (compare with **1c–e**), however the oxygenated derivatives **1l** and **1m** lost more than an order of magnitude in potency relative to

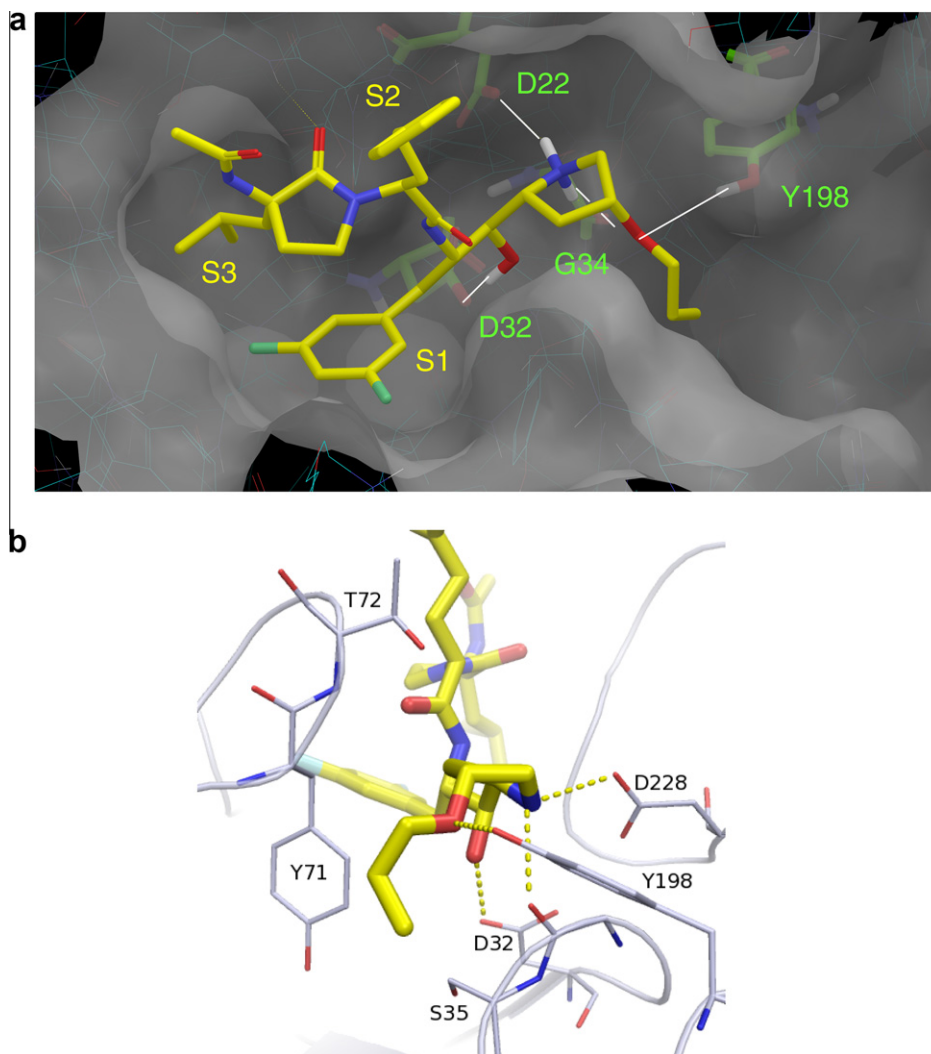
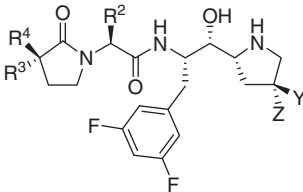
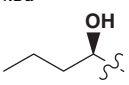
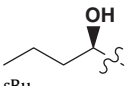
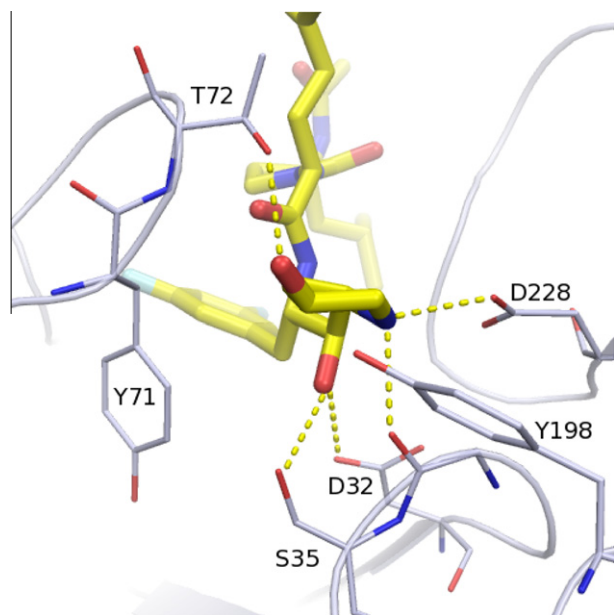


Figure 3. X-ray crystal structure of **28a** in the BACE-1 active site.

Table 3



Compound	R ⁴	R ³	R ²	Y	Z	HPLC ^a IC ₅₀ (nM)	HEKsw ^b IC ₅₀ (nM)
28l	NHAc	sBu	(CH ₂) ₂ Ph	H	OH	6.5	29
28m	H	nBu	(CH ₂) ₂ Ph	H	OH	25	650
28n	NHAc	sBu	(CH ₂) ₂ Ph	OH	H	0.89	11
28o	H	nBu	(CH ₂) ₂ Ph	OH	H	110	720
28p	H		(CH ₂) ₂ Ph	OH	H	16	220
28q	NHAc	sBu	Me	OH	H	31	>660
28r	H	nBu	Me	OH	H	96	1400
28s	H		Me	OH	H	40	870
28t	NHAc	sBu	(CH ₂) ₂ Ph	H	O ⁱ Ph	2.6	1.4
28u	NHAc	sBu	(CH ₂) ₂ Ph	H	O-2-pyridyl	2.6	2.1
28v	NHAc	sBu	(CH ₂) ₂ Ph	H	O-3-pyridyl	5.9	2.5
28w	H	nBu	(CH ₂) ₂ Ph	H	O-2-pyridyl	n.d.	360
28x	H	iBu	(CH ₂) ₂ Ph	H	O-2-pyridyl	n.d.	510
28y	H	iBu	Me	H	O-2-pyridyl	n.d.	330
29	NHAc	sBu	(CH ₂) ₂ Ph	H	NH ₂	34	270
30	NHAc	sBu	(CH ₂) ₂ Ph	NH ₂	H	50	190
31a	NHAc	sBu	(CH ₂) ₂ Ph	H	OBn	n.d.	12
31b	NHAc	sBu	(CH ₂) ₂ Ph	H	OCH ₂ (mCF ₃ C ₆ H ₄)	2.7	71
31c	NHAc	sBu	(CH ₂) ₂ Ph	H	OCH ₂ (mCNC ₆ H ₄)	3.0	4.2
31d	NHAc	sBu	(CH ₂) ₂ Ph	H	OCH ₂ (pFC ₆ H ₄)	10	8.9
31e	NHAc	sBu	(CH ₂) ₂ Ph	H	OCH ₂ (2-C ₅ NH ₄)	1.5	1.3
31f	NHAc	sBu	(CH ₂) ₂ Ph	H	OCH ₂ (3-C ₅ NH ₄)	1.4	2.0

^a n = 2.^b n = 4.Figure 4. Model of **28n** docked in to the BACE-1 active site.

their homophenylalanine congener (e.g., from 32 nM (**1f**) to 480 nM (**1i**)). Importantly, we observed that **1i** (60 nM) was essentially equipotent with the disubstituted lactam **1h** (46 nM) in vitro. Furthermore, **1i** was only sixfold less potent in vitro and eightfold less potent in the cells (81 nM) than the homophenylalanine disub-

Table 4

A β reduction and drug exposure in rat plasma and brain

Compound	Rat plasma A β % of control, ^a 5 h	Rat plasma exposure (nM), 5 h	Rat brain A β % of control, ^a 5 h	B/P ratio, 5 h
1i	26	1600	112	0.18
28c	23	4000	114	0.02

^a '% of control' = 100 – (% reduction in A β).

stituted lactam **1b** (11 nM in vitro, 10 nM in HEK cells). We viewed the modest loss in potency for **1i** compared to **1b** favorably, since **1i** had two fewer heteroatoms and 114 Da less molecular weight than **1b**. The in vivo profile of compound **1i** will be discussed later in this paper.

We then turned our attention toward increasing the potency of our analogs by introducing a conformational constraint within the 1,3-diaminopropan-2-ol fragment. As previously described,⁸ tying back the methoxybenzyl group into a tetrahydroisoquinoline (THIQ) afforded potent analogs **25a** and **26** (Table 2). In contrast to the acyclic analogs **1**, however, cellular potency diminished greatly (>10-fold) when combined with mono-substituted lactams (**25c–d**, 1400 and 720 nM cell IC₅₀'s, respectively). Nevertheless, the tolerance of the enzyme for the novel cyclic disubstituted lactams **25a** and **26** encouraged us to look for additional constrained templates, ideally with a lower molecular weight.

Removing the prime-side aryl group allowed us to focus on smaller nitrogen heterocycles. Molecular modeling suggested that the 4-hydroxypyrrolidine ring would be well tolerated, and the convenient handle at C(4) offered the potential for further

derivatization. Specifically, the propyloxypyrrolidine derivatives **28a–k** were the first compounds examined due to the predicted H-bonding interaction between Y198 and the C(4) ether oxygen as well as the hydrophobic interaction between the *n*-propyl group and Y71 (Fig. 2). The improved potency of the propyloxypyrrolidine disubstituted lactams **28a** and **28b** (Table 2, in vitro and cellular IC_{50} 's less than 3 nM) over the THIQ analogs **25a–b** and **26** demonstrated the superiority of the propyloxypyrrolidine isostere. The X-ray crystal structure of BACE-1 in complex with **28a**^{14–16} confirmed both the predicted Y198-OPr H-bond and the propyl ether hydrophobic contact with Y71 (Fig. 3). The group of mono-substituted lactams **28c–g** bearing various P3 groups were all more than 10-fold more potent in cells than the THIQ comparator **25c**. The *i*-butyl and (*R*)-1-hydroxybutyl analogs **28e** and **28g** were equipotent (~5 nM) to the disubstituted lactam **25a**, and only slightly less potent in vitro than **28a** and **28b**.

We reduced the molecular weight of our analogs further by trimming the P2 group to an alanine residue. As seen in our acyclic series, the potency of compounds **28h–k** was diminished (four- to 14-fold, depending on the pair examined). However, compound **28j** was among the smallest compounds studied (509 Da), and was a reasonably potent inhibitor of BACE-1 (HPLC IC_{50} = 35 nM).

Examination of molecular modeling suggested several additional analogs at the C(4) position of the pyrrolidine (Table 3). The (*R*)-4-hydroxy analog **28i** (6.5 nM) was threefold less active than its propyloxy congener **28b**, but a striking order-of-magnitude less potent in cells (29 nM). Consistent with our prior SAR, the corresponding monosubstituted lactam **28m** (R^4 = H) was less potent than the disubstituted lactam **28i** (R^4 = NHAc), again with a larger reduction in cellular potency than in vitro potency (>20-fold and 4-fold, respectively). Interestingly, the (*S*)-4-hydroxypyrrolidine analog **28n** was ~1 nM in vitro, but was only 11 nM in cells. Molecular modeling (Fig. 4) predicted a unique H-bond between the C(4)-OH and the T72 hydroxyl group on the enzyme's flap. This interaction may also explain the impressive selectivity of **28n** over other aspartyl proteases (3400- to 6000-fold over cathepsin D, cathepsin E, and pepsin), since T72 is not conserved in these enzymes. Compounds lacking the interaction with T72 are less selective (i.e., **28b**, 31- to 40-fold selective). Among the cohort of (*S*)-4-hydroxypyrrolidine monosubstituted lactams **28o–s**, comparator **28o** (R^3 = *n*-Bu) was the least potent (110 nM), while **28p** (R^3 = (*R*)-1-hydroxybutyl) was 16 nM. Additionally, the P2 alanine derivatives **28q** and **28s** were also more potent than **28r** (Table 3, 96 nM, R^3 = *n*-Bu). The subtle factors responsible for the detrimental effect of the P3 *n*-butyl substituent in this sub-series were not examined. The 4-aminopyrrolidine analogs **29** and **30** were each less potent than their hydroxyl counterparts.

Several additional ether groups at the (*R*)-C(4) were equipotent to the propyloxy parent **28b**, including the phenoxy and pyridoxy derivatives **28t–v**, however the monosubstituted analogs **28w–y** all were two orders of magnitude less potent in cells. Several benzylic ethers (**31a–f**) were also shown to be potent inhibitors of BACE-1, but did not contribute the additional potency needed to justify the added molecular weight.

To test our hypothesis that compounds of lower molecular weight would result in greater brain penetrance, we evaluated PK and PD effects in female CD-1GS rats.¹⁷ Monosubstituted lactams **1i** and **28c** were dosed at 30 mpk ip, and we determined both drug levels and %A β lowering 5 h post-dose (Table 4). Compound **1i** lowered plasma A β to 26% of control (74% A β reduction) with a peripheral exposure of 1.6 μ M (rat free fraction 2.9%,¹⁸ 46 nM free drug), in reasonable agreement with the cellular IC_{50} of 81 nM. Despite moderate central exposure of 270 nM (B/P 0.18) there was no effect on central A β levels. While we did not attempt to measure the % free drug in the brain, it appears that 270 nM total drug was not sufficient to cover the 81 nM free-drug IC_{50} at the target. This data suggests

that the lack of efficacy was likely a consequence of non-specific binding in the central compartment.¹⁹ The propyloxy-pyrrolidine analog **28c** demonstrated similar peripheral A β lowering to **1i**, however the negligible central exposure for this compound was disappointing. Although not determined for **28c**, several close analogs (**28a**, **28h**, and **28j**) were shown to be Pgp substrates in the bi-directional Caco-2 assay measuring the ratio of basolateral to apical permeability versus apical to basolateral permeability. The compounds **28a**, **28h**, and **28j** had ratios of >12, >17, and 32, respectively, indicating significant active transport.

Given the in vitro potency and selectivity of **28n**, we examined this compound in male Tg 2576 mice (30 mpk, sc).²⁰ At 5 h post-dose, we observed a modest reduction in plasma A β (66% of control) with a plasma concentration of 780 nM (Tg mouse % F_u = 10%, 78 nM free-drug). Although we didn't observe brain A β lowering, we were quite interested to see a high B/P ratio (0.87, 680 nM). To try to understand the disconnect between the exposure and lack of efficacy, a timecourse experiment was performed. Figure 5 shows that, while peripheral exposure declined over time in the expected fashion in conjunction with a return of peripheral A β to baseline, the central exposure remained ~800 nM over 12 h with no pharmacological effect seen at any timepoint. The reason for the prolonged retention of **28n** in the central compartment is unknown, but could involve non-specific binding to brain tissue or active transport since **28n** is a substrate for Mrp.²¹ Regardless of the mechanism, unbound drug levels in the brain of **28n** were

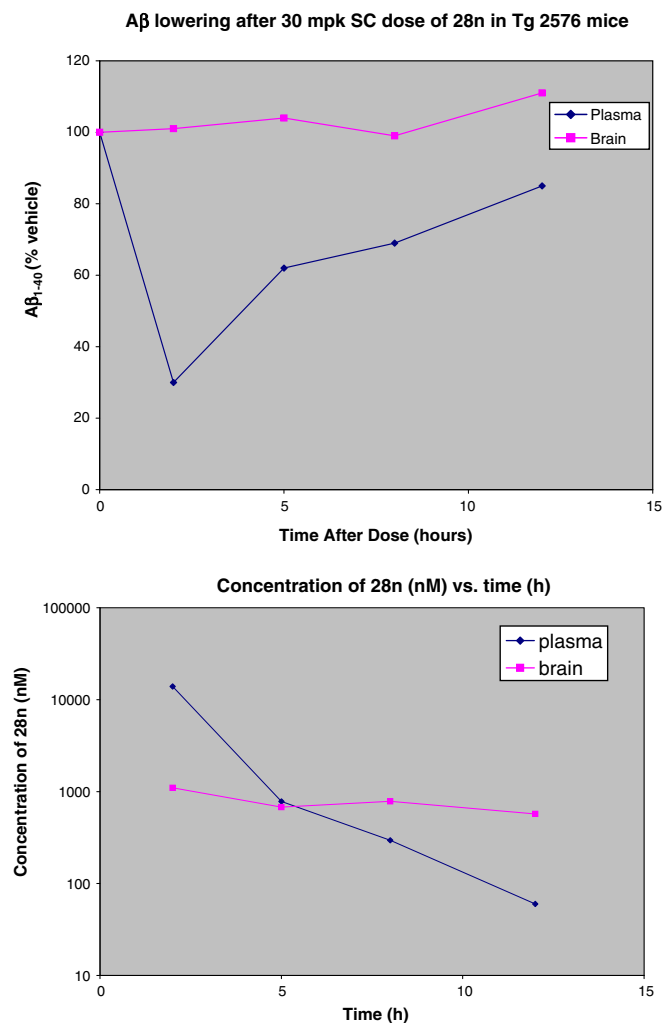


Figure 5. PK/PD of **28n** in Tg 2576 mouse plasma and brain.

insufficient to reduce brain A β . For a discussion of similar observations with additional potent BACE-1 inhibitors, see Ref. 13.

In summary, we discovered a class of potent BACE-1 inhibitors which were lower in molecular weight and heteroatom count than our lead compound **1a**. In animals, compound **1i** was efficacious in reducing plasma A β , but did not lower brain A β even though it has a molecular weight 22% less than **1a**. We also developed a versatile, constrained pyrrolidine template containing a 1,3-diaminopropan-2-ol isostere which exhibited improved potency versus its acyclic congeners. Specifically, the hydroxypyrrolidine **28n** was potent, exquisitely selective against other aspartyl proteases, and CNS penetrant. However, achieving A β lowering in the brain still remains a challenge, highlighted by the difficulty in obtaining central exposure from relatively small compounds such as **1i** and **28c** as a result of Pgp efflux, and additionally, what seems to be the high non-specific binding within brain tissues as seen for **28n**.

Acknowledgments

The authors appreciate the contributions of the following colleagues. Maria Pierdomenico, Kelli Jones, and Rudy Krause conducted the rat and mouse in vivo experiments while Tracey Fiedler and Jason Corsa executed the accompanying A β assays. Carol Krause and Cathy Kieras performed our HEK_{sw} assays. Paul Morin and Vidhyashankar Ramamurthy generated the BACE constructs used in crystallographic studies.

References and notes

- Maslow, K. *Alzheimer Dement.* **2008**, *4*, 110.
- Alzheimer's Foundation of America. <http://www.alzfdn.org/AboutAlzheimers/statistics.html> (accessed April 20, 2010).
- Palmer, A. M. *Trends Pharm. Sci.* **2002**, *23*, 426.
- Hardy, J.; Selkoe, D. J. *Science* **2002**, *297*, 353.
- Walsh, D. M.; Selkoe, D. J. *J. Neurochem.* **2007**, *101*, 1172.
- Zheng, H.; Koo, E. H. *Mol. Neurodegen.* **2006**, *1*, 5.
- DeStrooper, B.; Annaert, W. J. *Cell Sci.* **2000**, *113*, 1857.
- Thompson, L. A., III.; Shi, J.; Decicco, C. P.; Tebben, A. J.; Olson, R. E.; Boy, K. M.; Guernon, J. M.; Good, A. C.; Liauw, A.; Zheng, C.; Copeland, R. A.; Combs, A. P.; Camac, D. M.; Muckelbauer, J. K.; Lentz, K. A.; Grace, J. E.; Burton, C. R.; Toyn, J. H.; Marcinkeviciene, J.; Meredith, J. E.; Albright, C. F.; Macor, J. E. *Bioorg. Med. Chem. Lett.* **2011**, Accompanying Article.
- Thompson, L. A., III.; Boy, K. M.; Shi, J.; Macor, J. E. U.S. Patent 7,388,007, 2008.
- Decicco, C. P.; Tebben, A. J.; Thompson, L. A., III.; Combs, A. P. U.S. Patent 7,557,137, 2009.
- The co-crystal structure of the acyclic compound 4-amino-5-((S)-3-sec-butyl-1-((S)-1-((2S,3R)-3-hydroxy-4-(3-methoxybenzylamino)-1-phenylbutan-2-ylamino)-1-oxo-4-phenylbutan-2-yl)-2-oxopyrrolidin-3-ylamino)-5-oxopentanoic acid in BACE was used as the starting point for the substituted pyrrolidine models. Initial conformations of **28a** and **28n** were generated by manual manipulation of the acyclic compound to incorporate the hydroxypyrrolidine ring variants. Conformational sampling of the hydroxypyrrolidine was then carried out using MacroModel (version 9.8, Schrodinger LLC, New York, NY) with the OPLSAA-2005 forcefield. Conformations of the hydroxypyrrolidine ring were sampled, while the remainder of the molecule was fixed. The resulting conformations were then rigidly docked into the BACE/ligand active site using Glide (version 5.6, Schrodinger). Top scoring poses were minimized using the refine module of Prime (version 2.2, Schrodinger) and final models were selected based on low energy and visual inspection.
- Iben, L. G.; Kopcho, L.; Marcinkeviciene, J.; Zheng, C.; Thompson, L. A.; Albright, C. F.; Toyn, J. H. *Eur. J. Pharmacol.* **2008**, *593*, 10.
- Meredith, J. E., Jr.; Thompson, L. A., III.; Toyn, J. H.; Marcin, L.; Barten, D. M.; Marcinkeviciene, J.; Kopcho, L.; Kim, Y.; Lin, A.; Guss, V.; Burton, C.; Iben, L.; Polson, C.; Cantone, J.; Ford, M.; Drexler, D.; Fiedler, T.; Lentz, K. A.; Grace, J. E., Jr.; Kolb, J.; Corsa, J.; Pierdomenico, M.; Jones, K.; Olson, R. E.; Macor, J. E.; Albright, C. F. *J. Pharm. Exper. Ther.* **2008**, *3262*, 502.
- Co-crystals of BACE-1 and a peptidic statin¹⁵ were soaked with 1 mM **28a** in a stabilizing buffer of 35% PEG8 K, 0.2 M ammonium sulfate, 0.1 M sodium cacodylate pH 6.2 for 24 h.
- Kornacker, M. G.; Copeland, R. A.; Hendrick, J. P.; Lai, Z.; Mapelli, C.; Witmer, M. R.; Marcinkeviciene, J.; Metzler, W. J.; Lee, V. G.; Riexinger, D. J.; Muckelbauer, J. K.; Chang, C. J.; Camac, D. M.; Morin, P. E. U.S. Patent Application Publication 2,007,149,763.
- Coordinates for the complex of BACE-1 with inhibitor **28a** have been deposited in the Protein Data Bank (www.rcsb.org) under PDB ID 3R2F.
- Rat experiments were performed in a manner similar to those for mice. See Ref. 13.
- For free-fraction methods, see Ref. 13.
- Maurer, T. S.; DeBartolo, D. B.; Tess, D. A.; Scott, D. O. *Drug Metab. Dispos.* **2005**, *33*, 175.
- Tg 2576 mouse experiments were performed in a manner similar to those for wt-mice, utilizing the human 26D6 antibody in place of the murine 252Q8 antibody. See Ref. 13.
- Cellular IC₅₀ values were obtained in N2A cells with and without the Mrp inhibitor MK-571. Compound **28n** exhibited a threefold shift in potency.